Which is a significant contributor for outside of the plasmapause, an ionospheric filling or a leakage of plasmaspheric materials?: Comparison of He II (304 Å) images

I. Yoshikawa,[1] A. Yamazaki,[2] K. Yamashita,[3] Y. Takizawa,[4] and M. Nakamura[1]

Received 9 July 2002; revised 13 October 2002; accepted 18 October 2002; published 20 February 2003.

[1] The EUV imagery of the plasmasphere was taken by the He II (304 Å) scanner on 20–21 September 1998 after the first success on 9–10 September [*Nakamura et al.*, 2000]. Total amount of the plasma seen in the outside of the plasmapause is inconsistent between the first and the second images, although geomagnetic and solar conditions are almost the same. These plasmas are directly filled from the ionosphere or continuously leak from the plasmasphere. We conclude that the contribution of the plasma leakage from the plasmasphere is as significant as the contribution of the direct filling from the ionosphere even under a quiet/moderate geomagnetic condition. *INDEX TERMS:* 2768 Magnetospheric Physics: Plasmasphere; 2730 Magnetospheric Physics: Magnetosphere—inner; 2794 Magnetospheric Physics: Instruments and techniques; 2463 Ionosphere: Plasma convection; *KEYWORDS:* plasmasphere, EUV, Planet-B, helium ions, ionospheric filling, closed drift path

Citation: Yoshikawa, I., A. Yamazaki, K. Yamashita, Y. Takizawa, and M. Nakamura, Which is a significant contributor for outside of the plasmapause, an ionospheric filling or a leakage of plasmaspheric materials?: Comparison of He II (304 Å) images, *J. Geophys. Res.*, *108*(A2), 1080, doi:10.1029/2002JA009578, 2003.

1. Introduction

[2] In the classical framework, the ionosphere has been regarded as a steady and unique supplier not only for the plasmasphere but also outside the plasmapause. There were important studies for the ionospheric filling since early 1970s, both observations [*Park*, 1970; *Chappell*, 1974; *Carpenter and Anderson*, 1992] and theory or modeling [*Banks et al.*, 1971] which addressed various filling problems. (*Singh and Horwitz* [1992] reviewed various aspects of the refilling studies.) *Carpenter and Anderson* [1992] formulated the equatorial density as $(-800 + 1400t) \cdot L^{-4.5} + (1 - \exp(-\frac{L-2}{10}))$ [cm^{-3}] from ground-based observations where t is given in hours. This means that $1400 \cdot L^{-4.5}$ [cm^{-3}/hour] is the filling rate. Recently, *Lawrence et al.* [1999] conclude that the ionospheric filling at geosynchronous orbit occurs in two steps: 0.6–12 cm^{-3} d^{-1} for early- (<24 hours) filling and 10–50 cm^{-3} d^{-1} for later-time filling. Furthermore, *Su et al.* [2001] surveyed the dependence of filling rate on geomagnetic and solar activities. In these studies, plasmas in the outer plasmasphere were treated as ionospheric origin.

[3] However, recently it becomes well known that there is another contributor for outside the plasmapause. A significant amount of cold plasma peels off the main body of the plasmasphere even under quiet geomagnetic conditions [*Moldwin et al.*, 1994; *Matsui et al.*, 1999, *Yoshikawa et al.*, 2000]. Because the plasmasphere is formed by a balance between the dawn-to-dusk convection electric field and the corotation electric field [*Nishida*, 1966], a slight enhancement of the dawn-to-dusk electric field causes the plasmaspheric ions to convect toward the outer magnetosphere [*Matsui et al.*, 1999]. *Matsui et al.* [1999] reported that the plasmaspheric cold ions escape toward the dayside magnetopause continuously with a flux of 3.6×10^{25} [ions/s] independent of *Kp*, even though they assume that the ionospheric supply is not dominant.

[4] Conventional in-situ observation collects much information on density, composition, flux, and energy of plasmas, and has brought much progress in space physics. However, since it provides only local information which does not include the necessary global aspect of the whole plasmasphere, it is difficult to draw a definite conclusion on the above two issues: to establish a formula for the ionospheric filling and to quantify the plasma leakage from the plasmasphere.

[5] More recently, *Nakamura et al.* [2000] succeeded in the EUV (He II (304 Å)) imaging of the plasmasphere/plasmapause by an extreme ultraviolet (XUV) scanner boarded on the Planet-B spacecraft. *Yoshikawa et al.* [2000] examined the first EUV image shown in Figures 1a and 1c, and concluded that 2.9×10^{28} plasmaspheric He^+ ions were peeled off the main body of the plasmasphere for 12 hours (43200s). This quantity corresponds to a flux of 6.7×10^{24} ions/s, assuming the ratio of He^+/H^+ to be 0.1. Later, the NASA's IMAGE satellite found the striking features of the plasmasphere, convection tails, depleted regions and isolated magnetic flux tubes filled to higher He^+ density than their neighbors [*Sandel et al.*, 2001].

[1]Institute of Space and Astronautical Science, Kanagawa, Japan.
[2]Communications Research Laboratory, Tokyo, Japan.
[3]Department of Physics, Nagoya University, Nagoya, Japan.
[4]Institute of Physical and Chemical Research, Saitama, Japan.

0148-0227/03/2002JA009578$09.00

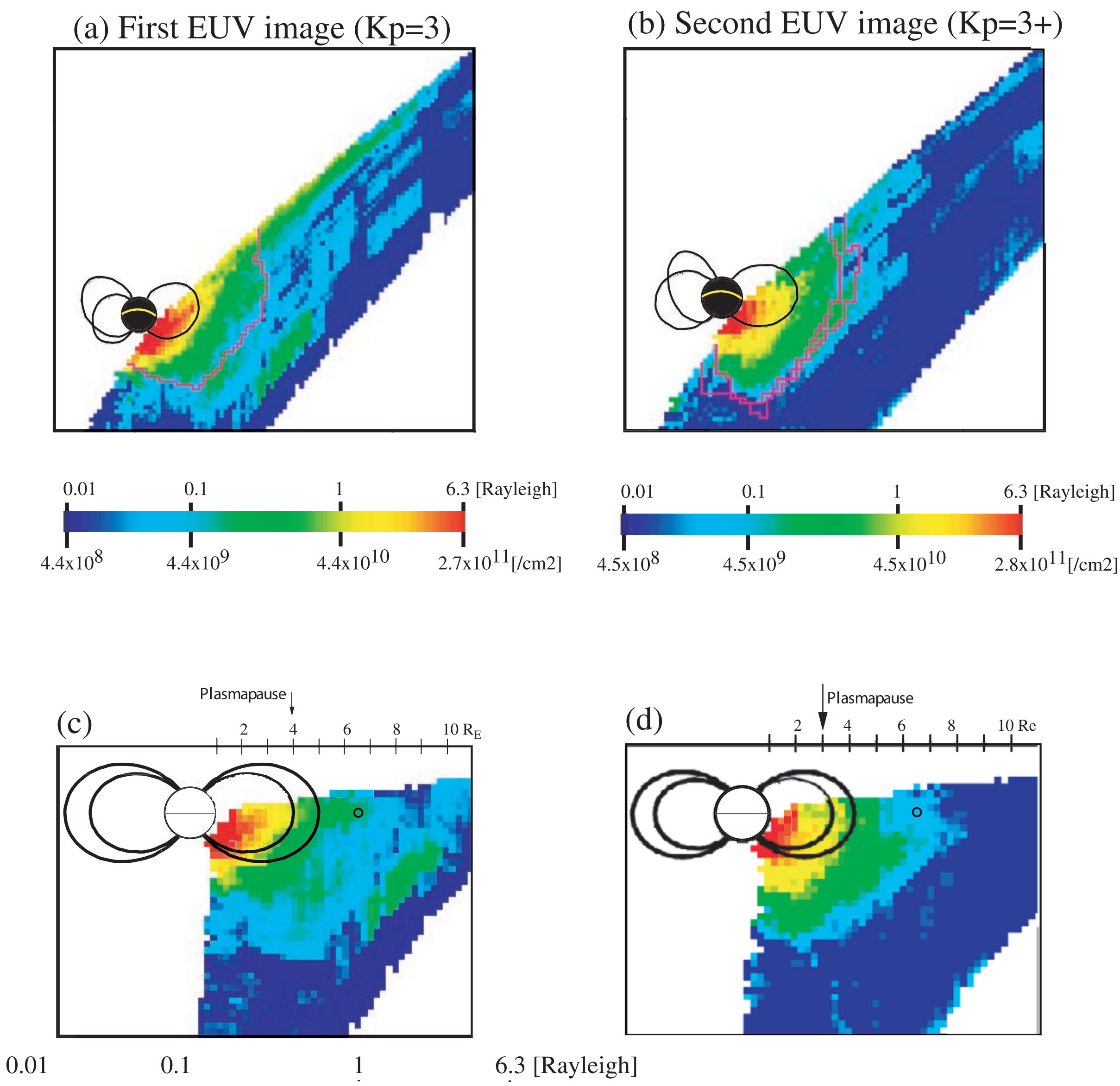

Figure 1. (a) Image of the plasmaspheric He II (304 Å) emission on September 9–10, 1998. The magnetic field lines of L = 4, whose foot points are 6, 12, 18 MLT, are superposed. The pink curve represents the outer shell of the OCDP under the corresponding IMF condition. (b) The same format as (a). Image on September 20–21, 1998. (c) Another perspective of (a) assuming the symmetrical shape of the plasmasphere. The dipole magnetic field lines of L = 4 and 5 are shown. (d) Another perspective of (b). The dipole magnetic field lines of L = 3 and 4 are shown.

[6] Their studies suggest that EUV images should provide promising clues for the verification of the above two topics, i.e., an ionospheric filling and a plasmaspheric leakage.

[7] In this paper, we will present the second EUV observation under a quiet/moderate geomagnetic condition (20–21 September 1998), which is similar to the previous observation (9–10 September 1998) [*Yoshikawa et al.*, 2000]. We examine the contributions of the plasmaspheric leakage and the ionospheric filling by comparing the two EUV images.

2. Instrumentation and Observation

[8] During this decade we have developed the EUV scanner for imaging planetary ionosphere/plasmasphere/magnetosphere [*Yoshikawa et al.*, 1997]. We built an extreme ultraviolet scanner (XUV) onboard Planet-B [*Nakamura et al.*, 1993, 1999; *Yoshikawa et al.*, 2001a]. The first Japanese Mars orbiter, Planet-B, was launched on July, 1998 and was in the parking orbit around the Earth for a few months. The orbit around the Earth provided us good perspective for imaging the plasmasphere.

[9] Figure 1a is a novel plasmaspheric He II (304 Å) image on 9–10 September discussed by *Yoshikawa et al.* [2000]. During this observation, the IMF data shows a clear dawnward tendency. A pink curve in Figure 1a represents the outer boundary of a corotational flow region. (The calculation method for this curve is described in the next section.) The sharp gradient of the electron density was seen

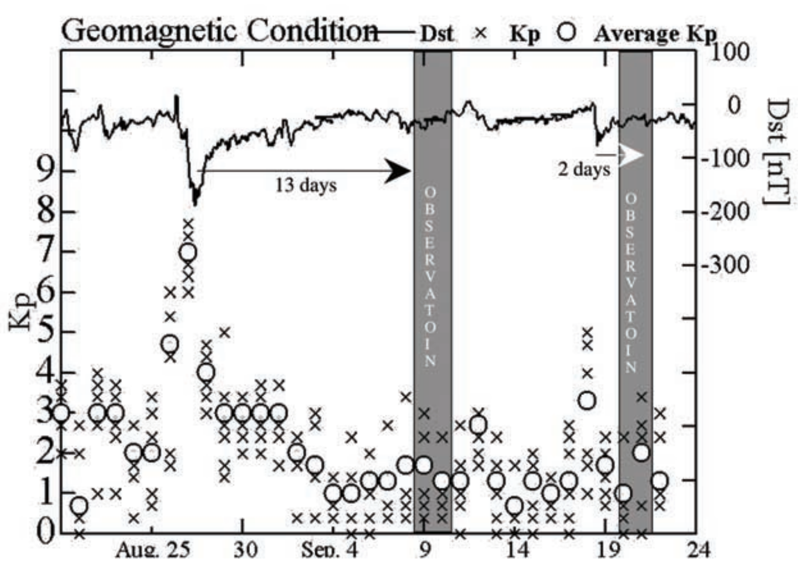

Figure 2. Long-term history of *Kp* index (cross), the daily averaged *Kp* (open circle), and *Dst* values (solid line) from the end of August 1998. Magnetic storms occurred on August 27 and September 18.

at L = 4 from the upper hybrid frequency observed by the Plasma Wave and Sounder (PWS) experiment onboard the EXOS-D satellite.

[10] The *Kp* index and *Dst* values since the end of August, 1998 are given in Figure 2. The crosses represent the *Kp* index, and the open circles are the daily averaged *Kp*. The *Dst* values are given as a solid line.The geomagnetic activity was quiet or moderate, and the maximum *Kp* was 3. The latest storm before the observation occurred on 27 August. The minimum *Dst* reached −155nT and the recovery phase lasted until 4 September.

[11] After the first success, we had the second opportunity for imaging the plasmasphere on 20 September 1998. Figure 3 shows the orbit during the two observations. Hatched regions indicate the imaging areas. At this time, the XUV scanner was turned on at 1610 UT on 20 September immediately after the magnetopause crossing of the spacecraft, and the XUV scanned the duskside of the plasmasphere. As *Yoshikawa et al.* [2000] noted previously, the XUV scanner has two channels (P- and L-channels), each of which has identical field-of-view (FOV) and different sensitivity. Since no prominent difference was found between the P- and L-channel data, we superposed P- and L-channel data into one picture shown in the Figure 1b which increased the quality of the image. All the procedures for the conversion of the raw data into the digitalized image are exactly the same as in the previous analysis [*Yoshikawa et al.*, 2000].

[12] The solar EUV flux is estimated from the ground-based observation of *F*10.7. In the second (first) observation, the *F*10.7 value was 136 (145) $\times 10^{-22}$ Wm^{-2} Hz^{-1}, and the corresponding solar 304 Å flux was 9.9×10^9 (10.0×10^9) photons · cm^{-2} sec^{-1}. The emission rate factor for He II (304 Å) is given to be 2.2×10^{-5} (2.3×10^{-5}) sec^{-1} particle^{-1}. The corresponding column density of helium ions is given at the color bar in the figures.

[13] The series of the *Kp* index, *Dst* values, and IMF conditions covering the second observation period and a 12-hour period prior to that are displayed in Figure 4. The IMF *By*/*Bz* angle (θ_{IMF}) and the IMF magnitude in the GSM YZ plane ($B_T = \sqrt{By^2 + Bz^2}$) from Geotail observation are displayed in the two upper panels. Data with 3-sec time resolution is represented by dots, while the open circles represent the data averaging the previous 40 minutes. The IMF data shows a clear duskward tendency, $\theta_{IMF} \sim 90°$. The geomagnetic activity was quiet or moderate with the maximum *Kp* of 3+. No large storm event was observed, since the last storm occurred on 18 September with the minimum *Dst* of −76 nT shown in Figure 2. Therefore, we conclude that the second EUV observation was done under the geomagnetic and solar conditions similar to the first observation. The sharp gradient of the electron density was identified at L = 3 by PWS on EXOS-D.

[14] Here we assume a symmetric structure of the duskside plasmasphere around the Z_{SM} axis, and plot tangential points along line-of-sight on the plane. (See Figure 4 of *Yoshikawa et al.* [2000].) Figures 1c and 1d are another perspective of Figures 1a and 1b, respectively. The dipole magnetic field lines are also displayed. The plasmapauses identified by PWS matched to the outer boundaries of the yellow regions.

[15] There are some similarities between the first and second observations. The maximum intensities of the plasmaspheric He II (304 Å) were about 10 Rayleigh which is consistent with the theoretical prediction by *Roelof et al.* [1992]. Significant amounts of plasma were found outside the plasmapause in both observations. A comparison of the first and second observations, however, clarifies the quantity of plasma outside the corotational flow region in the second observation was several times smaller than that in the first EUV image, even though both images were taken under similar solar and geomagnetic conditions. (See outside of pink curves in Figures 1a and 1b.)

[16] The plasmapause seen in the EUV images is not a sharp boundary but a gentle slope. This is a proof that the plasmaspheric materials continuously leak to the outside of

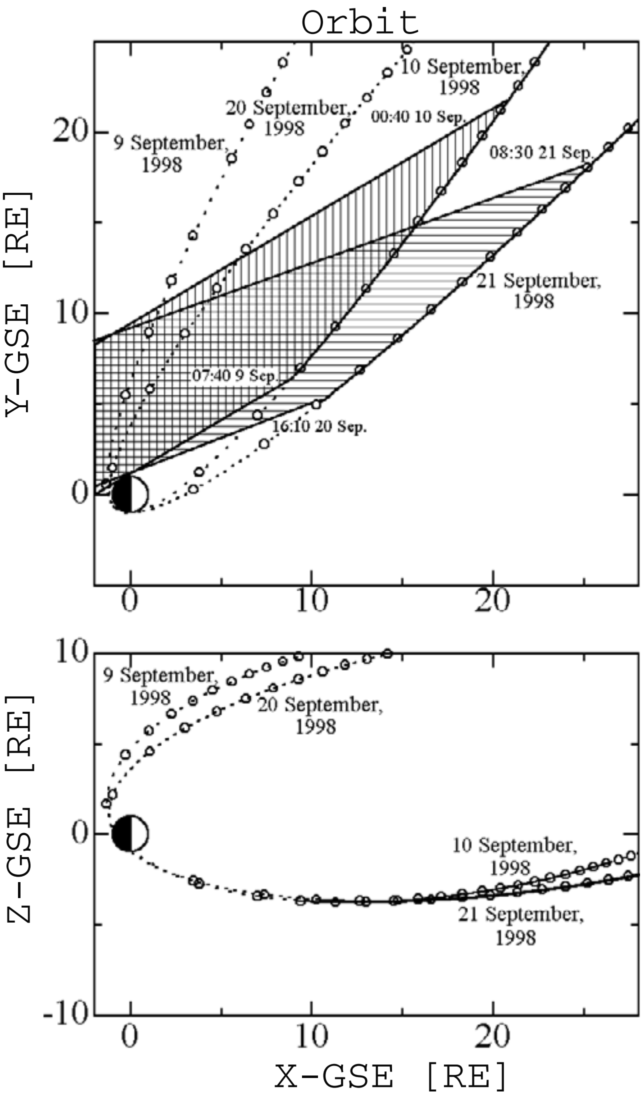

Figure 3. Planet-B orbit in geocentric solar-ecliptic (GSE) coordinate for the second imaging opportunity, which is superposed on the orbit of the first observation. Hatched regions indicate the imaging areas.

duskside plasmasphere, because these images are not instantaneous snapshots but accumulated images for hours.

3. What Makes a Difference?

[17] The pink curves in Figures 1a and 1b represent the outermost closed drift path of a flux tube (OCDP) boundaries. It must be noted that the OCDP does not always correspond to the plasmapause, but it is the outer boundary of a corotational flow region. Thus, cold plasmas inside the OCDP are considered to corotate around the Earth, and are not convected to the outer region. In order to determine the shape of the OCDP boundary, we at first calculate the motions of flux tubes in the equatorial plane. The electric field structure used here is the empirical high-latitude potential model by *Weimer* [1996] with interplanetary magnetic field data from Geotail. Potential patterns by the Weimer's model mapped out to the geomagnetic equatorial plane by using Tsyganenko model [*Tsyganenko*, 1989]. The $E \times B$ drifts of convecting flux tubes are calculated and we determine the OCDP. (We presented the details of the OCDP boundary in Figure 1a in another publication [*Yoshikawa et al.*, 2001b].)

[18] As for the first observation, the north/duskward IMF condition ($B_T = 6$ nT, $\theta_{IMF} = 315°$) is used in the calculation of OCDP, as described by *Yoshikawa et al.* [2001b].

[19] As for the second observation, we used two IMF conditions in calculation to meet the reality. One condition demonstrates the former half of the observation representing the parameters of $B_T = 2$ nT and $\theta_{IMF} = 90°$, and the other is the latter half of the observation with $B_T = 6$ nT and $\theta_{IMF} = 90°$. In the latter condition, the OCDP is located closer to the Earth, as indicated by the inner pink line. It is clear that the significant difference between the two images appears in the outside of OCDPs and this difference cannot be explained by the different IMF conditions.

4. Ionosphere is Not a Unique Contributor for Plasma Outside OCDP

[20] If the ionosphere is a unique and dominant source for cold plasma outside the OCDP, there must be always a constant amount of plasma in this region while the solar flux is constant which is true for our observations. The difference in the He II (304 Å) emission intensity between two images suggests that the ionosphere is not an only contributor for cold plasma outside the OCDP and we should consider that the plasmas are peeled off from the plasmasphere in addition/instead. This should be a promising proof that significant amount of the plasmaspheric materials leak toward the outer magnetosphere even under quiet to moderate conditions, as has recently been discussed [*Matsui et al.*, 1999; *Moldwin et al.*, 1994].

[21] Based on the discussion above, let us estimate the contribution of the plasmaspheric ions leaked to the outside of OCDPs. Figure 5 illustrates a possible leakage process of plasmaspheric ions, as *Matsui et al.* [1999] proposed. The convection drift paths based on *Weimer* [1996] and *Tsyganenko* [1989] models are superimposed. The large blue disk represents the plasmasphere ($L < 4$). The yellow and red areas are originally corotation-dominant regions where the plasmas circulate around the Earth. The IMF parameters generally fluctuate, which lead to a small variation of a convection electric field. The induced small enhancement in the electric field causes the original OCDP to shrink at the duskside. As a result, the plasmas in the outer part of the corotation-dominant region indicated as the red area are forced to move toward the outer magnetosphere. Keeping this scenario in mind, we deduce the following from the EUV images and the in-situ measurements.

1. From Figures 1a and 1b, we calculate the total amounts of cold helium ions outside the OCDPs in the first and second observations. The quantity of the cold helium ions in the first observation was about five times larger than that in second observation; 1.2×10^{29} ions and 2.3×10^{28} ions, respectively.

2. The solar flux during the two observations are almost the same according to $F10.7$ values; The ionospheric filling rates should be the same in two observations. Hereinafter, the amount of helium ions by the ionospheric filling to the

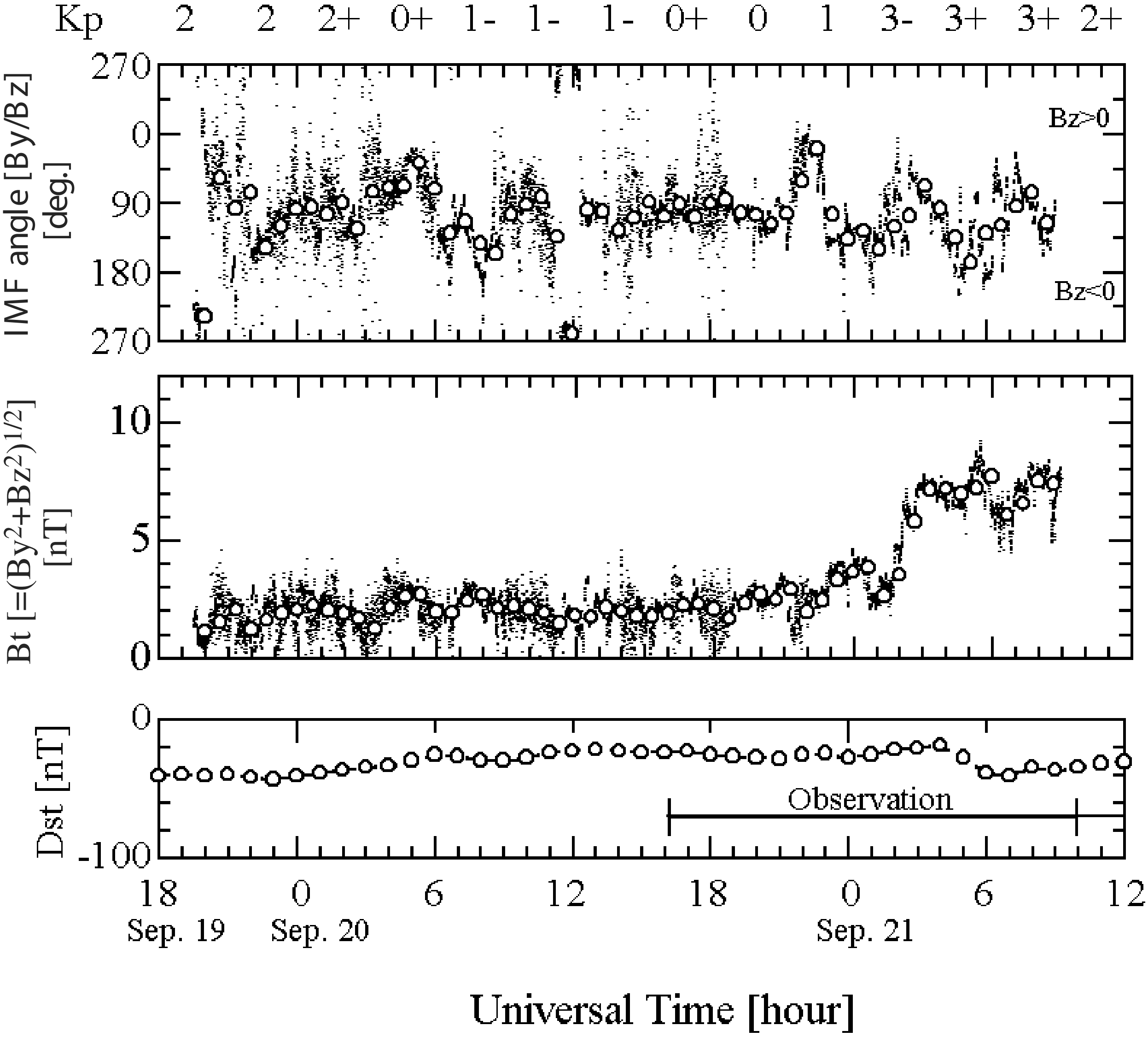

Figure 4. Geomagnetic and the IMF conditions. The series of *Kp* index, *Dst* values, and interplanetary magnetic field (IMF) condition covering the observation period (+ a previous 12-hour period) are displayed. Geomagnetic activity was quiet or moderate, and maximum *Kp* was 3+. The IMF had a duskward direction. No storm was identified.

outside of the OCDP is referred as x [ions]. The quantities of the plasmaspheric leakage are given as $1.2 \times 10^{29} - x$ [ions] for the first observation and $2.3 \times 10^{28} - x$ [*ions*] for the second observation. Figure 6 schematically illustrates this situation.

3. The total amount of plasma within the OCDP in the first observation was considered to be larger than that in the second observation. Electron densities deduced from PWS onboard EXOS-D along the nearly identical satellite's paths indicate the electron density at $L = 4.3$ in the first observation was about 100 cm^{-3} at 14.4 MLT, which was 16.6 times higher than that of the second one, about 6 cm^{-3} at 15.6 MLT. (Average of these two values is consistent with the predicted density of 30 cm^{-3} [*Carpenter and Anderson*, 1992].)

[22] It should be noted that in both observations the location at $L = 4.3$ around 15 MLT was very close to the OCDP boundary, but inside the OCDP boundary. The distances between the in-situ observation points and OCDP boundaries was less than 0.2 R_E. Such geometric configuration is shown in Figure 5, where the location of in-situ measurement is given as a dot. (The use of in-situ measurement is the best way to know the density just inside OCDP. Because LOS in Figure 5 cuts the region outside OCDP (red) as well as that inside OCDP (yellow). Otherwise LOS contains the quantity of the plasmasphere.)

[23] If the fluctuated components of the dawn-to-dusk electric field during the two observations are not considerably different, the stagnation point would fluctuate in a similar manner. When we adopt the above assumption for a

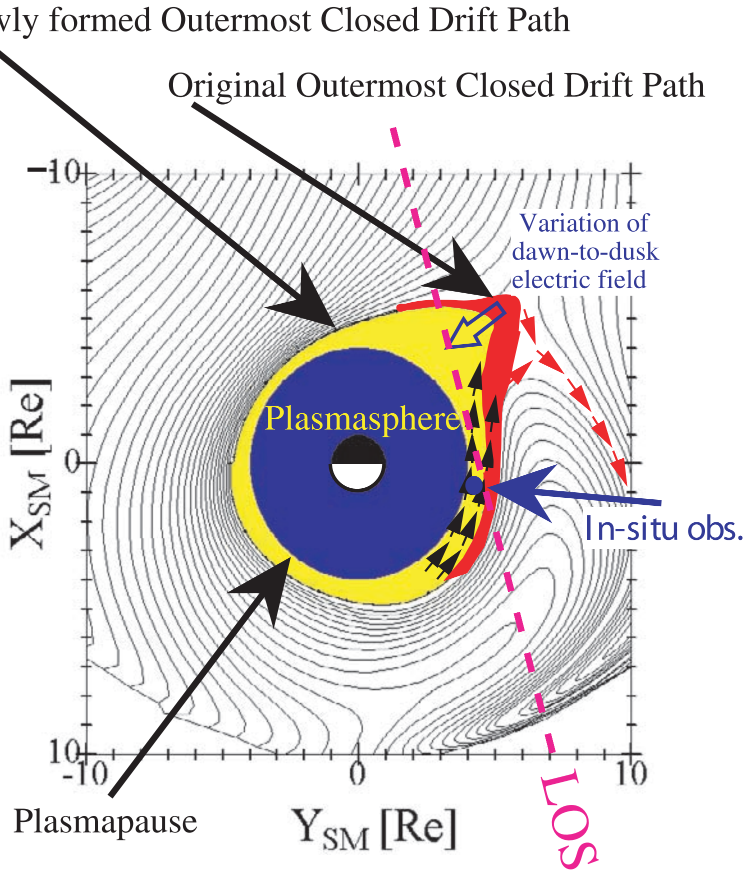

Figure 5. Schematic diagram of leakage plasmas. During steady convection electric field conditions, the region inside the OCDP but outside the plasmapause, which is indicated as yellow and red areas, continues to corotate around the Earth and is filled up to high densities. Even a small enhancement of convection electric field causes a stagnation point to move inward and a part of the plasma originally in the corotational region, indicated as the red area, leaks to the outer magnetosphere.

simplicity, then we can infer the following conclusion: "The total amount of plasma, which peeled off from the inside of the OCDP, is proportional to the density inside the OCDP."

[24] This conclusion provides the following relation, if we assume that the ratios of He^+ ions to electron densities in both observations are the same.

$$1.2 \times 10^{29} - x : 2.3 \times 10^{28} - x = 16.6 : 1 \tag{1}$$

[25] We obtain $x = 1.7 \times 10^{28}$ cm^{-2}. Hence, the contribution of plasmaspheric leakage to the total plasma in each observation, ξ, is calculated as

$$\xi_{\text{first}} = \frac{1.2 \times 10^{29} - x}{1.2 \times 10^{29}} = 0.86, \quad \xi_{\text{second}} = \frac{2.3 \times 10^{28} - x}{2.3 \times 10^{28}} = 0.26 \tag{2}$$

[26] The former value means that during the first observation, 86 percent of the plasma outside the OCDP was originated from the plasmasphere, and the ionospheric filling effect was smaller (14 percent). The latter value means that during the second observation, 26 percent of plasma outside the OCDP was plasmaspheric materials and the rest (74 percent) was from the ionosphere.

[27] In the above argument, we imply that the density inside the OCDP influences the total amount of plasma

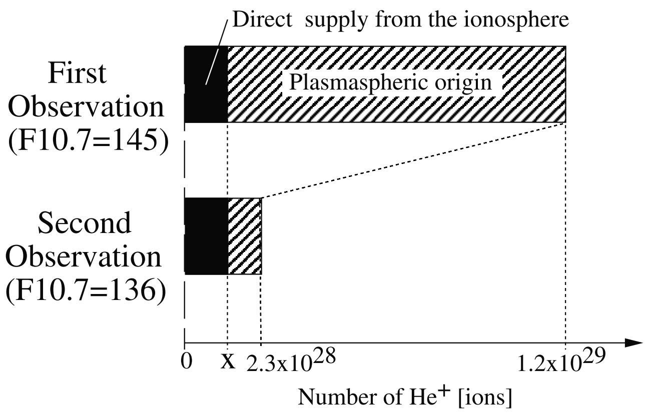

Figure 6. Bar graph of total helium ion outside the OCDP. The EUV image in the first observation found the cold helium ions outside the OCDP five times as much as that of the second observation.

outside the OCDP. Namely, the amount of plasma outside the OCDP depends on how much the plasmasphere is filled up with cold plasma. As shown in previous section, magnetic storms occurred on 27 August 27 and 18 September. The first observation (9 September 1998) started 13 days after the first storm. There are theoretical and experimental reports that plasmasphere is filled up in 4–5 days [*Carpenter and Anderson*, 1992; *Rasmussen et al.*, 1993]. According to these reports, the plasmasphere was considered to be already filled up by the first observation. On the contrary the second observation was only 2 days after the storm, and the plasmasphere was not expected to be filled up to high density. We conclude that total amount of plasma outside OCDP depends on the filling level of the plasmasphere. But this is not an exclusive conclusion. Further analysis is needed by using more EUV images.

[28] *Yoshikawa et al.* [2001b] reported that the first EUV image gives the best fit to an ad-hoc model where a filling rate has an L^{-3} dependence, instead of the well-known L^{-4} density dependence. Namely, more gentle slope than L^{-4} is considered to be due to an additional materials of the plasmaspheric leakage, while the direct filling from the ionosphere has an L^{-4} dependence on flux tube volume.

[29] Finally, we compare the filling quantity obtained in this study with those from recent reports based on in-situ measurements. *Lawrence et al.* [1999] reported that the early-time filling rate at geosynchronous orbit (L = 6.6) is 0.6–12 cm^{-3} d^{-1}. *Su et al.* [2001] reported a smaller variation of the early-time filling rate, 2.5–6.5 cm^{-3} d^{-1}. Based on their results, we evaluate the corresponding column density by the following equation.

$$Clmn(He^+) = \int_{LOS} \left(\int_{halfday} Fr \cdot dt \right) \left(\frac{L}{6.6} \right)^{-4} dl \qquad (3)$$

Fr is the filling rate reported by *Lawrence et al.* [1999] and *Su et al.* [2001]. $\int_{half\,day} dt$ means that a flux tube is filled for a half day. L^{-4} density dependence on flux tube volume is assumed. *dl* is a segment along Line-Of-Sight (LOS) of the observation. Here we also assume the ratio of He^+/H^+ to be 0.1, therefore we employ 0.06–1.2 cm^{-3} d^{-1} or 0.25–0.65 cm^{-3} d^{-1} as *Fr*. Then, $Clmn(He^+)$ is calculated as $7.0 \times 10^7 \sim 1.4 \times 10^9$ ions/cm^2 and $0.29 \times 10^9 \sim 0.76 \times 10^9$ ions/cm^2, which correspond to *Lawrence*'s and *Su*'s values, respectively.

[30] On the other hand, the column densities of He^+ ions around L = 6.6 are 7.7×10^9 ions/cm^2 for the first observation and 1.5×10^9 ions/cm^2 for the second observation (See circles in Figures 1c and 1d). Therefore, subtracting the contribution of the plasmaspheric leakage in equation (2), we have the column densities of He^+ due to the ionospheric filling, 1.08×10^9 ions/cm^2 for the first observation and 1.11×10^9 ions/cm^2 for the second observation. Therefore, the ionospheric contribution deduced from our EUV imagery is consistent with those from recent in-situ observations.

5. Summary

[31] We discussed the second EUV observation on 20–21 September 1998 and found the similar, as well as the different aspects in the EUV images between the first and the second observations. The maximum intensities of plasmaspheric He II (304 Å) in two observations were found to be about 10 Rayleigh and are consistent with the theoretical prediction by *Roelof et al.* [1992]. If we consider the core dense region as the plasmasphere, the locations of the plasmapause are in good agreement with those identified by the in-situ measurements.

[32] The significant amount of the plasma was found outside a corotational flow region in the two observations. These plasmas are directly filled from the ionosphere or continuously leak from the plasmasphere. We conclude that the contribution of the plasma leakage from the plasmasphere is as significant as the contribution of the direct filling from the ionosphere even under a quiet/moderate geomagnetic condition.

[33] **Acknowledgments.** The authors thank all members of Planet-B project team for their remarkable efforts leading to the success of Planet-B. We used IMF data from the magnetic field instrument (MGF) onboard Geotail. The data is available via the scientific data base (DARTS) constructed mainly by the ISAS PLAIN CENTER. We thank to T. Nagai who is a principal investigator for the MGF instrument.

[34] Arthur Richmond thanks Jiannan Tu and another reviewer for their assistance in evaluating this paper.

References

Banks, P. M., A. F. Nagy, and W. I. Axford, Dynamical behavior of thermal protons in the mid-latitude ionosphere and magnetosphere, *Planet. Space Sci.*, *19*, 1053, 1971.
Carpenter, D. L., and R. R. Anderson, An ISEE/Whistler model of equatorial electron density in the magnetosphere, *J. Geophys. Res.*, *97*, 1097, 1992.
Chappell, C. R., Detached plasma regions in the magnetosphere, *J. Geophys. Res.*, *79*, 1861, 1974.
Lawrence, D. J., F. M. Thomsen, J. E. Borovsky, and D. J. Comas, Measurements of early and late-time plasmasphere refilling as observed from geosynchronous orbit, *J. Geophys. Res.*, *104*, 14,691, 1999.
Matsui, H., T. Mukai, S. Ohtani, K. Hayashi, R. C. Elphic, M. F. Thomsen, and H. Matsumoto, Cold dense plasma in the outer magnetosphere, *J. Geophys. Res.*, *104*, 25,077, 1999.
Moldwin, M. B., M. F. Thomsen, S. J. Bame, D. J. McComas, and K. R. Moore, An examination of the structured and dynamics of the outer plasmasphere using multiple geosynchronous satellites, *J. Geophys. Res.*, *99*, 11,475, 1994.
Nakamura, M., T. Yamamoto, K. Tsuruda, Y. Saito, K. Yamashita, A. Furuzawa, T. Ogawa, and S. Chakrabarti, Interplanetary He II extreme-ultraviolet observation on PLANET-B, *Opt. Eng.*, *32*, 3033, 1993.
Nakamura, M., et al., Helium observation in the Martian ionosphere by an X-ray ultraviolet scanner on Mars orbiter NOZOMI, *Earth Planet. Space*, *51*, 61, 1999.
Nakamura, M., I. Yoshikawa, A. Yamazaki, K. Shiomi, Y. Takizawa, M. Hirahara, K. Yamashita, Y. Saito, and W. Miyake, Terrestrial plasmaspheric imaging by an extreme ultraviolet scanner on Planet-B, *Geophys. Res. Lett.*, *27*, 141, 2000.
Nishida, A., Formation of plasmapause, or magnetospheric plasma knee, by the combined action of magnetospheric convection and plasma escape from the tail, *J. Geophys. Res.*, *71*, 5669, 1966.
Park, C. G., Whistler observations of the interchange of ionization between the ionosphere and the protonosphere, *J. Geophys. Res.*, *75*, 4249, 1970.
Rasmussen, C. E., S. M. Guiter, and S. G. Thomas, A two-dimensional model of the plasmasphere: Refilling time constants, *Planet. Space Sci.*, *41*, 35, 1993.
Roelof, E. C., B. H. Mauk, and R. R. Meier, Instrument requirements for imaging the magnetosphere in extreme-ultraviolet and energetic neutral atoms derived from computer-simulated images, *SPIE*, *1744*, 19, 1992.
Sandel, R., A. King, T. Forrester, L. Gallagher, L. Broadfoot, and C. Curtis, Initial results from the IMAGE Extreme Ultraviolet Imager, *Geophys. Res. Lett.*, *28*, 1439, 2001.
Singh, M., and J. L. Horwitz, Plasmasphere refilling: Recent observations and modeling, *J. Geophys. Res.*, *97*, 1049, 1992.
Su, Y., M. F. Thomsen, J. E. Borovsky, and D. J. Lawrence, A comprehensive survey of plasmasphere refilling at geosynchronous orbit, *J. Geophys. Res.*, *106*, 25,615, 2001.

Tsyganenko, N. A., A magnetospheric magnetic field model with a warped tail current sheet, *Planet. Space Sci.*, *37*, 5, 1989.

Weimer, D. R., A flexible, IMF dependent model of high-latitude electric potentials having ‘‘space weather’’ applications, *Geophys. Res. Lett.*, *23*, 2549, 1996.

Yoshikawa, I., M. Nakamura, M. Hirahara, T. Takizawa, K. Yamashita, H. Kunieda, T. Yamazaki, K. Misaki, and A. Yamaguchi, Observation of He II emission from the plasmasphere by a newly developed EUV telescope onboard sounding rocket S-520-19, *J. Geophys. Res.*, *102*, 19,897, 1997.

Yoshikawa, I., A. Yamazaki, K. Shiomi, K. Yamashita, Y. Takizawa, and M. Nakamura, Evolution of the outer plasmasphere during low geomagnetic activity observed by the EUV scanner onboard Planet-B, *J. Geophys. Res.*, *105*, 27,777, 2000.

Yoshikawa, I., A. Yamazaki, K. Shiomi, M. Nakamura, K. Yamashita, Y. Saito, M. Hirahara, Y. Takizawa, W. Miyake, and S. Matsuura, Development of a compact EUV photometer for imaging the planetary magnetosphere, *J. Geophys. Res.*, *106*, 26,057, 2001a.

Yoshikawa, I., A. Yamazaki, K. Shiomi, K. Yamashita, Y. Takizawa, and M. Nakamura, Interpretation of the He II (304 Å) EUV image of the inner magnetosphere by using empirical models, *J. Geophys. Res.*, *106*, 25,745, 2001b.

M. Nakamura and I. Yoshikawa, Institute of Space and Astronautical Science, 3-1-1 Yoshinodai, Saganihara, Kanagawa 229-8510, Japan. (mnakamur@stp.isas.ac.jp; yosikawa@stp.isas.ac.jp)

Y. Takizawa, Cyclotron Laboratory, Institute of Physical and Chemical Research, Saitama 351-0198, Japan. (takky@riken.go.jp)

K. Yamashita, Department of Physics, Nagoya University, Nagoya 464-8602, Japan.

A. Yamazaki, Communications Research Laboratory, Tokyo 184-8795, Japan. (yamachan@crl.go.jp)